# Two-quasiparticle structures and isomers in $^{168}$Er, $^{170}$Er, and $^{172}$Er

G. D. Dracoulis,[1,*] G. J. Lane,[1] F. G. Kondev,[2] H. Watanabe,[3] D. Seweryniak,[4] S. Zhu,[4] M. P. Carpenter,[4] C. J. Chiara,[2,†] R. V. F. Janssens,[4] T. Lauritsen,[4] C. J. Lister,[4] E. A. McCutchan,[4] and I. Stefanescu[4,5]

[1]*Department of Nuclear Physics, R.S.P.E, Australian National University, Canberra ACT 0200, Australia*

[2]*Nuclear Engineering Division, Argonne National Laboratory, Argonne, Illinois 60439, USA*

[3]*RIKEN Nishina Center, 2-1 Hirosawa, Wako, Saitama 351-0198, Japan*

[4]*Physics Division, Argonne National Laboratory, Argonne, Illinois 60439, USA*

[5]*Department of Chemistry and Biochemistry, University of Maryland, College Park, Maryland 20742, USA*

(Received 2 March 2010; published 20 May 2010)

The stable and neutron-rich isotopes $^{168}$Er, $^{170}$Er, and $^{172}$Er have been studied with Gammasphere using inelastic excitation with energetic $^{136}$Xe beams. The previously assigned structures based on the proposed $K^\pi = 4^-$ isomeric intrinsic states in both $^{168}$Er and $^{170}$Er have been re-evaluated and an equivalent band identified in $^{172}$Er. In $^{170}$Er, the identification of a $K^\pi = 6^-$ band with transitions close in energy to those of the $4^-$ band leads to a modified interpretation, since the overlap would have compromised previous analyses. The $g_K - g_R$ values for the $4^-$ bands deduced from the in-band $\gamma$-ray intensities for the sequence of isotopes suggest a predominantly two-neutron configuration in $^{168}$Er, an equally mixed two-neutron, two-proton configuration in $^{170}$Er, and a two-proton configuration in $^{172}$Er. A comprehensive decay scheme for the previously proposed $6^+$ isomer in $^{172}$Er has also been established, as well as band structures built on this isomer that closely resemble the $6^+$ and $7^-$ two-neutron structures known in the isotone $^{174}$Yb. The implied $K$ hindrances are discussed. The main decay path of the $6^+$ isomer occurs through the newly identified $4^-$ isomer. The measured lifetimes of the $4^-$ and $6^+$ isomers in $^{172}$Er are 57(3) and 822(90) ns, respectively. Multiquasiparticle calculations support the suggested configuration changes across the isotopic chain.

DOI: 10.1103/PhysRevC.81.054313 PACS number(s): 21.10.Re, 23.20.Lv, 23.35.+g, 27.70.+q

## I. INTRODUCTION

The stable even-even isotopes $^{168}$Er and $^{170}$Er are not accessible with heavy-ion induced fusion evaporation reactions, but they have been studied extensively, mainly through $\beta$-decay, neutron capture, and inelastic neutron scattering, as well as through Coulomb and inelastic excitation, and multinucleon transfer with heavy ions [1–5]. Unlike the higher-$Z$ even-even isotopes near stability, where isomers are common, only a single long-lived state is known in each of the isotopes $^{168}$Er and $^{170}$Er, both suggested to have $K^\pi = 4^-$. Their associated rotational bands have recently been identified and analyzed [3]: the conclusion reached was that they arise predominantly from the parallel coupling of the $1/2^-[521]$ and $7/2^+[633]$ neutron orbitals in $^{168}$Er, but from the $1/2^+[411] \otimes 7/2^-[523]$ two-proton configuration in $^{170}$Er, although there were residual issues with the comparison between measured $g_K - g_R$ values and the pure Nilsson values. In comparison, very little is known about intrinsic excitations in the neutron-rich isotope $^{172}$Er. Its ground-state rotational band was identified in two-neutron transfer studies with $^{238}$U beams [5], while a proposed $K^\pi = 6^+$ isomer, with an approximate lifetime in the microsecond region, was identified in our spectroscopic studies with similar reactions induced by $^{136}$Xe beams [6]. One aim of the present work was to characterize the proposed $6^+$ isomer in $^{172}$Er by using a more prolific reaction, but also to obtain more comprehensive information on other excited states to probe the relationship between the two-neutron and two-proton configurations in the sequence of even-even erbium isotopes. The new results include the extension and clarification of the $^{168}$Er and $^{170}$Er schemes and the characterization of two isomers in $^{172}$Er. The results are discussed in terms of the structures anticipated from multiquasiparticle calculations.

## II. EXPERIMENTAL PROCEDURES

The experimental techniques used are essentially identical to those reported in a series of studies aimed at the spectroscopy of stable and neutron-rich well-deformed nuclei near $Z \sim 70$ (see, for instance, Refs. [6–8]). The beam and target conditions in these experiments (with beam energies ~20% above the Coulomb barrier) result in inelastic processes with single and multiple transfer of nucleons as well as inelastic excitation of the target and projectile nuclei [9–12].

Pulsed and chopped beams of 830-MeV $^{136}$Xe were provided by the Argonne Tandem-Linac Accelerator System (ATLAS) facility at Argonne National Laboratory. $\gamma$ rays were detected with the Gammasphere array [13] and various timing conditions were used to identify isomers and to allow isolation of specific structures using $\gamma$-$\gamma$-time correlations. The beams were incident on a 6 mg/cm$^2$ thick metallic foil, enriched in $^{170}$Er, and placed on a 25 mg/cm$^2$ gold backing. Under these conditions, $\gamma$ rays from very short-lived states will exhibit attenuated Doppler shifts, thus limiting the identification of

*Corresponding author; george.dracoulis@anu.edu.au

†Present address: Physics Division, Argonne National Laboratory, Argonne, Illinois 60439, USA, and Department of Chemistry and Biochemistry, University of Maryland, College Park, Maryland 20742, USA.

 

high-spin states, unless they are populated through isomers, in which case the final decays will come from nuclei at rest. In contrast, the measurements of Wu *et al.* [3] used thin targets and coincidences with projectile-like and target-like fragments for channel selection, resulting in the identification of higher-spin states, but with lower energy resolution (≈1.1%) than in the present work.

Our main measurements used nanosecond pulses, separated by 856 ns, with a requirement to detect at least three $\gamma$ rays with a relative time difference within the ±850 ns range. About $6 \times 10^8$ coincidence events of three-fold and higher were collected in this configuration. A sequence of measurements were made as well with macroscopically chopped beams with beam-on/beam-off conditions that ranged from the microsecond to the seconds regime (as in Ref. [8]). In these measurements, data were only collected in the out-of-beam time region with a dual $\gamma$-$\gamma$-time condition applied. The latter measurements did not result in the identification of any very long-lived isomers in the nuclei of interest.

## III. ANALYSIS TECHNIQUES

While the nonselective nature of the reaction process means that a broad range of nuclei and nuclear states is excited, the ability to use different time and $\gamma$-ray energy gating conditions results in flexibility and high sensitivity. A variety of time conditions constraining both the time difference between specific $\gamma$ rays, and their time relative to the beam pulses, can be exploited. Recent developments in software [14] have allowed very efficient production of coincidence matrices with such differing constraints.

## IV. RESULTS AND LEVEL SCHEMES

### A. Transition strengths

Selected transition strengths that will be useful in the level scheme assignments are given in Table I. Those for decays from the $4^-$ isomers in $^{168}$Er and $^{170}$Er have been partly covered previously [3] and will not be repeated in full here, but a more complete set for $^{170}$Er is included in the table. The reduced hindrance factors $f_\nu$ are also listed, where appropriate. The hindrance $F$ is the inverse of the transition strength in Weisskopf units, and the reduced hindrance is defined by $f_\nu = F^{1/\nu}$. The degree of forbiddenness for a multipolarity $\lambda$ is given by the shortfall between the required $K$ change and the transition multipolarity, $\nu = \Delta K - \lambda$. Except for the case of $E1$ transitions, which are already inhibited, typical values of $f_\nu$ range between about 50 and several hundred.

From earlier studies, the $4^-$ isomer in $^{168}$Er at 1094 keV had a precisely measured mean life of 157(1) ns [1], and a

TABLE I. Transition strengths and hindrances for decays from isomers in $^{170}$Er and $^{172}$Er.

| $E_\gamma$ (keV) | $I_\gamma$ [a] relative | $\sigma\lambda$ | $\alpha_T$ | $B(\sigma\lambda)$ ($e^2$ fm$^{2\lambda}$ or $\mu_0^2$ fm$^{(2\lambda-2)}$) | Strength (W.u.) | $\nu$ | $f_\nu$ [b] |
|---|---|---|---|---|---|---|---|
| $^{170}$Er; 1269 keV; $\tau$ = 63(2) ns; $K^\pi = 4^-$ | | | | | | | |
| 51.3 | 6.8(5) | $E1$ | 0.355 | $3.91(35) \times 10^{-6}$ | $1.98(18) \times 10^{-6}$ | 0 | |
| 141.5 | 4.6(6) | $E1$ | 0.129 | $1.26(18) \times 10^{-7}$ | $6.37(90) \times 10^{-8}$ | 1 | *16000* |
| 165.3 | 10.2(7) | $E1$ | 0.086 | $1.76(15) \times 10^{-7}$ | $8.86(76) \times 10^{-8}$ | 0 | |
| 258.1 | 100(5) | $E1$ | 0.027 | $4.52(33) \times 10^{-7}$ | $2.28(17) \times 10^{-7}$ | 1 | *4400* |
| 1008.3 | 0.25(8) | $E1$ | 0.00135 | $1.9(6) \times 10^{-11}$ | $0.96(31) \times 10^{-11}$ | 3 | *471* |
| $^{170}$Er; 1591 keV; $\tau$ = 5.7(15) ns; $K^\pi = 6^-$ | | | | | | | |
| 94.5 | 900(31) | $M1$ | 3.350 | $2.38(64) \times 10^{-3}$ | $1.33(36) \times 10^{-3}$ | 1 | 763 |
| 218.3 | 460(17) | $M1$ | 0.316 | $9.7(26) \times 10^{-5}$ | $5.43(15) \times 10^{-5}$ | 1 | 18409 |
| 322 | <16 | $E2$ | 0.056 | <0.146 | $<2.6 \times 10^{-3}$ | 0 | |
| $^{170}$Er; 1591 keV; $\tau$ = 5.7(15) ns; $K^\pi = 7^-$ | | | | | | | |
| 94.5 | 900(31) | $M1$ | 3.350 | $2.38(64) \times 10^{-3}$ | $1.33(36) \times 10^{-3}$ | 2 | 27 |
| 218.3 | 460(17) | $E2$ | 0.189 | 30(8) | 0.53(14) | 1 | 1.9 |
| $^{172}$Er; 1501 keV; $\tau$ = 822(90) ns; $K^\pi = 6^+$ | | | | | | | |
| 133.6 | 355(12) | $E1$ | 0.1507 | $2.17(26) \times 10^{-7}$ | $1.09(13) \times 10^{-7}$ | 1 | *9180* |
| 970.5 | 22(3) | $M1$ | 0.0066 | $3.18(56) \times 10^{-10}$ | $1.78(32) \times 10^{-9}$ | 5 | 56 |
| 369.7 | 43(3) | $E2$ | 0.0373 | $1.18(16) \times 10^{-2}$ | $2.07(28) \times 10^{-4}$ | 2 | 69 |
| 249.6 | 40(3) | $M1$ | 0.219 | $3.40(46) \times 10^{-7}$ | $1.90(26) \times 10^{-7}$ | 3 | 174 |
| $^{172}$Er; 1263 keV; $\tau$ = 57(3) ns; $K^\pi = 4^-$ | | | | | | | |
| 229.1 | 88(6) | $E1$ | 0.0366 | $2.61(23) \times 10^{-7}$ | $1.31(12) \times 10^{-7}$ | 1 | *7600* |
| 1008.3 | 218(6) | $E1$ | 0.00135 | $7.58(50) \times 10^{-9}$ | $3.80(25) \times 10^{-9}$ | 3 | *64* |

[a] Relative intensities from the present work except for those from the $4^-$ band in $^{170}$Er which are from the data compilations [2].

[b] Values in italics include an additional factor of $10^3$ in the expected single-particle hindrance for $E1$ transitions. $f_\nu$ is not defined for $\nu = 0$, and $f_\nu = F$ when $\nu = 1$; see text for details.

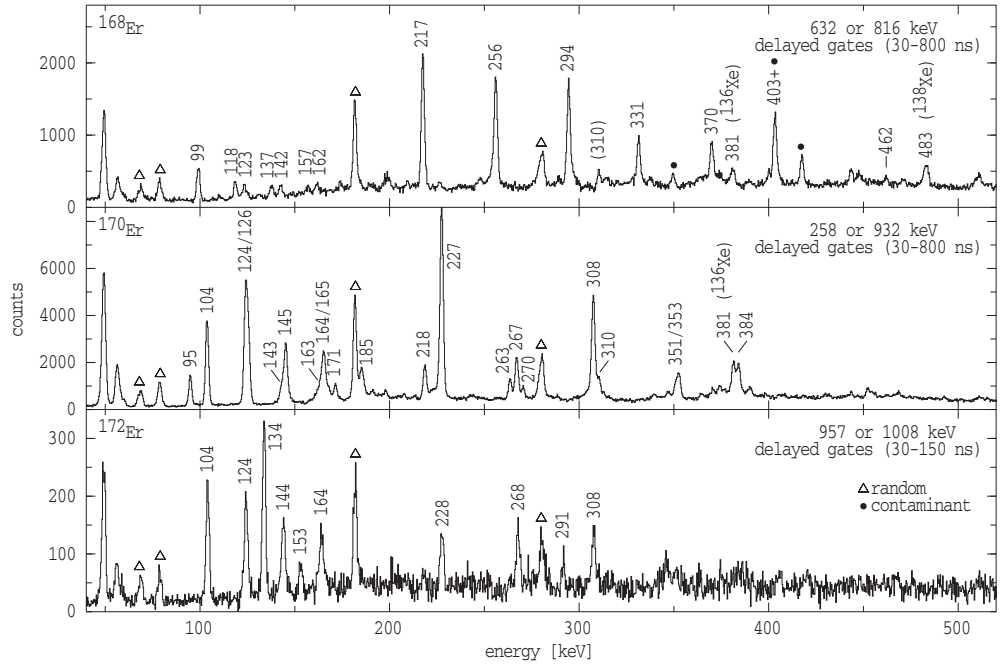


FIG. 1. Time-correlated $\gamma$-$\gamma$ coincidence spectra selecting transitions feeding the proposed $4^-$ isomers, with energy and time gates as indicated.

consistent but less precise value of $\tau = 159(8)$ ns is obtained in the present measurements. For $^{170}$Er, a value equivalent to $\tau = 61.8(25)$ ns was reported in Ref. [3], and our result of $\tau = 63(2)$ ns is in good agreement. No other isomers with significant lifetimes, except for the ∼6 ns state found in $^{170}$Er in the present work, have been identified in either of these two isotopes. As will be shown later (Sec. IV D), together with the relatively long-lived isomer proposed previously, a new $4^-$ isomer has also been identified in $^{172}$Er, with $\tau = 57(3)$ ns. The main transitions which feed the $4^-$ isomers in each isotope are evident in the spectra of Fig. 1 constructed with gates on the most intense delayed lines that follow the isomeric decays in each isotope. [Note that these have different time gates, and that additional results for $^{172}$Er related to the higher-lying isomer will be discussed later (Sec. IV D)].

These spectra are indicative approximately of the relative yields of the three isotopes. The nuclide $^{168}$Er (top panel) is populated both by inelastic excitation of the residual $^{168}$Er isotope in the enriched target (∼1.5%) and two-neutron transfer from $^{170}$Er to the projectile, hence the presence of lines from mutual excitation of $^{136}$Xe and $^{138}$Xe, respectively. (Note that the main $^{136}$Xe line at 1313 keV is out of range in these spectra.) As expected, the most intense excitation is that of $^{170}$Er (middle panel), while $^{172}$Er (bottom panel) is an order of magnitude weaker. The complementary partner in the $^{172}$Er case is $^{134}$Xe, whose main lines are at 847 and 884 keV (see Sec. IV D and Fig. 6).

### B. $^{168}$Er

A partial level scheme showing only those states significantly populated in the present study is given in Fig. 2. The $4^-$ band identified by Wu *et al.* [3] is confirmed, but with more precise energies and with direct observation of the $(I \rightarrow I-1)$ cascade transitions up to the decay of the $9^-$ state. These were not observed in Ref. [3] because of the lower sensitivity in those measurements (the uppermost panel of Fig. 1 can be compared with Fig. 2 of Ref. [3]), although some transitions were known from the earlier studies [1].

The present results provide an independent measure of the in-band branching ratios that can be used to probe the configuration of the $4^-$ structure, as will be discussed later. The $(6^-)$ band (right of Fig. 2) was also not observed in Ref. [3], but several of its lower states were known [1] and they are independently identified here from the $\gamma$-$\gamma$ coincidence measurements.

### C. $^{170}$Er

The level scheme deduced for $^{170}$Er is presented in Fig. 3. The results for the $4^-$ band are partly in agreement with those given by Wu *et al.* [3], but the better energy resolution and higher sensitivity leads to some significant additions to the scheme with implications for branching ratio measurements.

Although it is probably a result of different state populations between the present work and that of Ref. [3], we cannot confirm the extension of the odd-spin states above the 1989.9-keV, $9^-$ level which continues with a 444-, 539-keV $E2$ cascade in the work of Ref. [3]. In the present study, while there is significant population of the even-spin sequence, at least up to the $12^-$ state above which Doppler broadening is a limitation, the population above the $7^-$ state in the odd-spin sequence must drop rapidly. This difference is evident in the spectrum showing prompt transitions feeding the isomer (middle panel, Fig. 1): compare, for example, the low intensity of the 267-keV, $7^- \rightarrow 5^-$ transition to that of the 308-keV,

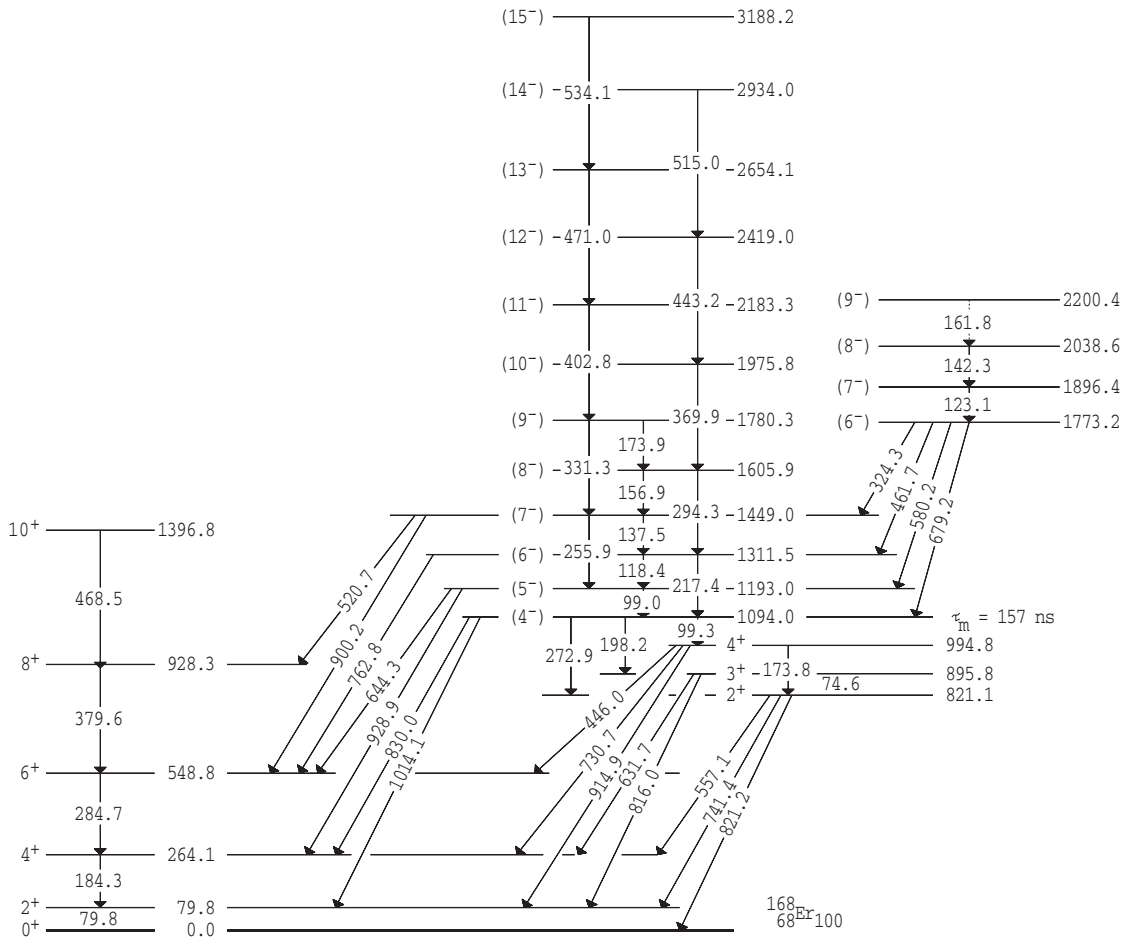


FIG. 2. Partial level scheme for $^{168}$Er as observed in the present study.

$8^- \rightarrow 6^-$ transition. This difference presumably implies that the main population path in this case is either directly or indirectly via $E2$ excitation from lower-spin states, given that the odd-spin excitation must proceed initially through the 104-keV $M1/E2$ transition which will be weaker than an $E2$ excitation from the $4^-$ bandhead to the even-spin states. Note also that the 351- and 353-keV transitions evident in the same spectrum are assigned (on the basis of the coincidence results) to transitions feeding the 1591-keV state, and not to transitions in the $4^-$ band.

It should also be noted that the 1638.9-keV, $7^-$ state assigned in the present work with out-of-band decays directly to the ground-state band, is several keV lower in energy than the 1640.5-keV, $(7^-)$ state listed in the evaluated nuclear data [2] as a member of the $4^-$ band. That state was assigned in Ref. [15] on the basis of 1100.0(1)- and 725.3(1)-keV branches to the $6^+$ and $8^+$ states, respectively, of the ground-state band. The branches we observe (in the $\gamma$-$\gamma$ coincidence data) are at 1098.8(2) and 724.3(3) keV, and we also identify the $\Delta I = 1$ and $\Delta I = 2$ in-band transitions whose energies match the present excited state energy. Figures 4(b) and 4(c) were constructed with double coincidence gates on either the 308- or 267-keV transitions in combination with the 258- and 932-keV $\gamma$ rays that are the main decays immediately following the $4^-$ isomer. They show the even- and odd-spin population clearly, and they also isolate the $6^- \rightarrow 5^-$ transition at 123.9 keV.

The last point is related to an important feature of the new scheme: the identification of a band based on the 1590.6-keV state, which branches into both the $6^-$ and $5^-$ levels of the $4^-$ band. This 1590.6-keV level was not observed in Ref. [3], but it was known [2,15], and it is independently confirmed here. The 95- and 218-keV connections to the $4^-$ band are clear in Fig. 1 (middle panel) and also in the double-gated spectra of Figs. 4(a) and 4(d). The band built on this state is identified in the present work, with dominant cascade transitions at 125.5, 145.1, and 165.4 keV. These would not have been resolvable from the 123.9-, 142.9-, and 164.2-keV transitions in the $4^-$ band in the work of Ref. [3], but they are, in fact, more intense. (The branching ratios will be discussed in a later section.)

The 1590.6-keV state was tentatively assigned [2,15] as $J^\pi = (6^-)$ and it was suggested [15] to be a bandhead arising from the $\nu 7/2^+[633] \otimes 5/2^-[512]$ configuration. The transition energies within the band are similar to those of the possible $6^-$ band in $^{168}$Er. However, while the negative parity is defined by the conversion coefficient for the 95-keV transition which indicates $M1$ multipolarity [2], the multipolarity of the 218-keV $\gamma$ ray has not been measured, but its $\gamma$-ray intensity is

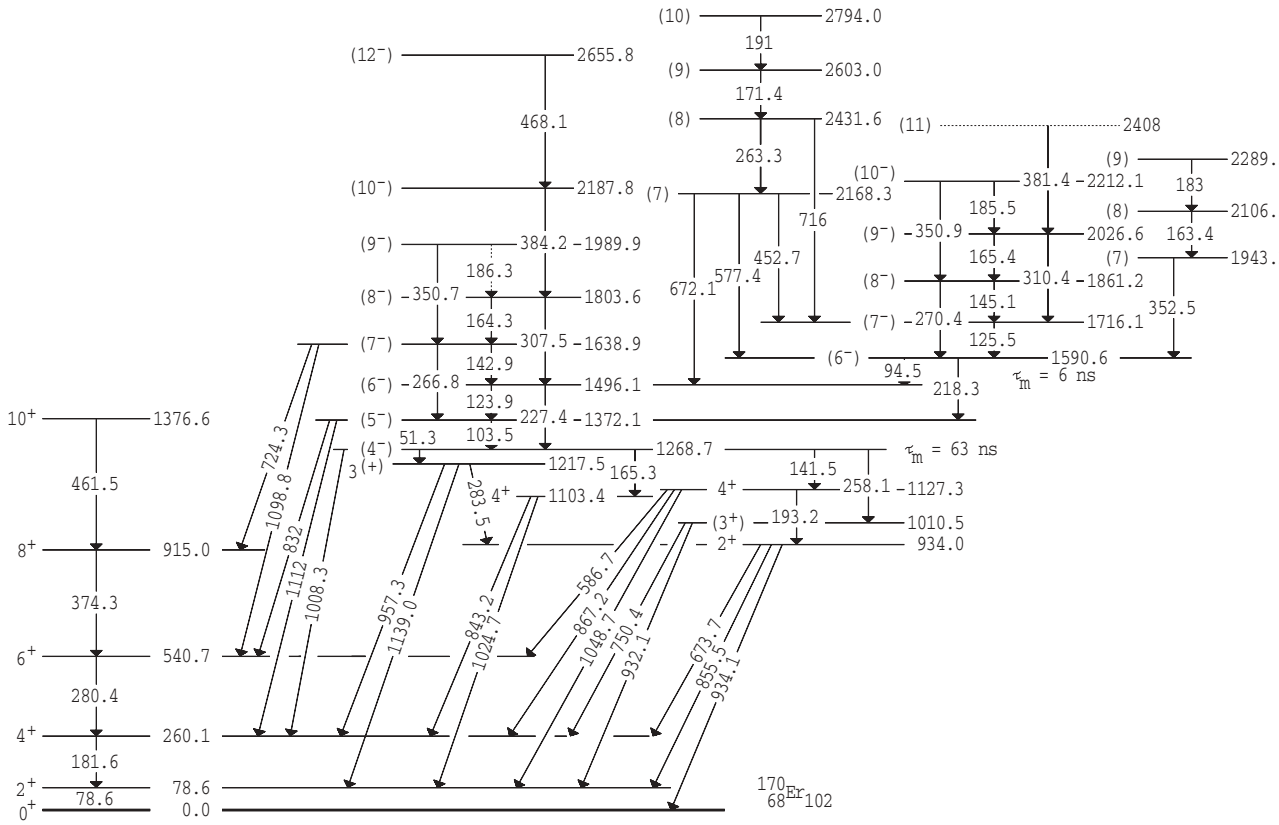


FIG. 3. Partial level scheme for $^{170}$Er as observed in the present study.

only half that of the 95-keV line. If both were of $M1$ multipolarity, the 218-keV transition would be favored by a factor of 12 by the $E_\gamma^3$ factor. This observation and the absence of an $E2$ transition directly to the $4^-$ state (discussed in detail directly below) argue against the $6^-$ possibility and in favor of a $K^\pi = 7^-$ assignment. (Compare, for contrast, the observed branching ratios for decays from the 1773-keV, $6^-$ state in $^{168}$Er.)

The mean life of $\tau = 5.7(1.5)$ ns obtained in the present work from a fit to the intermediate time spectrum constructed with gates on the transitions in the band, and either the 218- or 227-keV transitions that follow, confirms the intrinsic nature of the state. Considering the arguments above, in the context of the transition strengths given in Table I, for a $K^\pi = 6^-$ assignment, the 95- and 218-keV transitions would have strengths of $1.3(4) \times 10^{-3}$ and $5.4(2) \times 10^{-5}$ W.u., while the limit on the possible 322-keV, $E2$ decay (with a $\gamma$-ray intensity that is $<1.7\%$ of that of the 95 keV transition) corresponds to an $E2$ strength of $<2.6 \times 10^{-3}$ W.u. This is a low value, and while there is a configuration change, such a transition would not be $K$-forbidden.

The strengths for the alternative $7^-$ assignment are given in Table I. In this case, the 218-keV line would be a once-forbidden $E2$ transition, but now its strength is unexpectedly high at 0.53(14) W.u. This can, at least partly, be explained by mixing between the 1591-keV state and the 1639-keV $7^-$ member of the $4^-$ band. As is well known (see Ref. [16]), a small admixture of a collective component can induce a significant component into an otherwise forbidden $E2$ transition. Following Ref. [16], the amplitude of the admixed component of the $K = 4$ state into the $K = 7$ level can be obtained from the ratio of the observed $B(E2)$ probabilities to that of an equivalent collective rotational transition within the $K^\pi = 4^-$ band, via the relation $\beta^2 = B(E2)_{218}/B(E2)^{\text{coll.}}$ with $B(E2)^{\text{coll.}} = (5/16\pi)Q_0^2| < IK20|I - 2K > |^2$. Assuming $Q_0 = 7.6\ e$ b leads to a collective $B(E2)$ of $7.02 \times 10^3 e^2$ fm$^4$. Our measured strength of the 218-keV transition is 30(8) $e^2$ fm$^4$, implying $\beta = 0.065$. Use of the relation that $V = \beta\sqrt{1-\beta^2}\Delta E$ then leads to the estimate of the mixing matrix element $|V| = 3.1$ keV. This is consistent with expectations for such matrix elements that are expected [16] to decrease as a function of the difference in $K$, the present difference being relatively small at $\Delta K = 3$.

There are remaining issues here, however, in that the primary test of this scenario (which assumes that there would be no transitions in the absence of mixing) is that the relative intensities of the $M1$ and $E2$ transitions from the $7^-$ isomer should match those of equivalent transitions within the $4^-$ band, which are controlled by the $g_K - g_R$ values of the $4^-$ configuration. The $g_K - g_R$ values will be discussed in detail later, but the 95-keV, 218-keV branching ratio corresponds to a larger $g_K - g_R$ value than that characteristic of the $4^-$ band, the 95-keV $\gamma$ ray being more intense than expected. This might not be a significant discrepancy in this case, since the absolute strength of the 95-keV $M1$ transition is still low at $\sim 1.3 \times 10^{-3}$ W.u., so there could be a component of significant relative intensity (say half) that is *not* from the mixing.

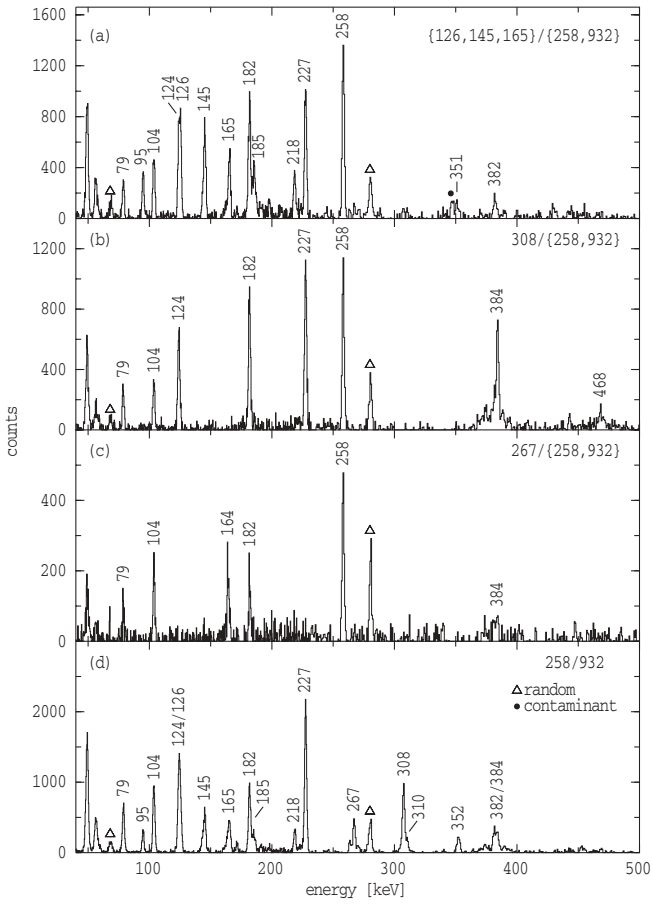


FIG. 4. Selected coincidence spectra for $^{170}$Er with double energy gates as indicated. A relative time condition of ±150 ns is applied.

An additional problem arises, however, with the $\log ft$ values measured in the $\beta$ decay of $^{170}$Ho. Although tentatively assigned as $J^\pi = (6^+)$, the $^{170}$Ho parent is almost certainly from the $\pi 7/2^-[523]\otimes\nu 5/2^-[512]$ configuration. Because of the relatively fast $\beta$ transition to the 1591-keV state ($\log ft$ value of 6.4), Ref. [15] attributed the decay to the one-particle transition $\pi 7/2^-[523]\rightarrow \nu 7/2^+[633]$, with the $5/2^-[512]$ neutron being a spectator, leading to the $6^-$ configuration. The $7^-$ proposition outlined above would involve, in addition, a change of the neutron orbital, a transition which would normally be very inhibited [17].

It seems therefore, that there is an incompatibility between the $\gamma$-ray decay properties and the $\beta$-decay population that remains to be resolved. A tentative $(6^-)$ assignment is retained in the present scheme, but both possibilities will be covered in the subsequent analysis of band properties. As will be shown later, the multiquasiparticle calculations suggest that both the $6^-$ and $7^-$ two-neutron configurations will be close in energy in the case of $^{170}$Er, hence a differentiation is not possible on theoretical grounds.

### D. $^{172}$Er

Previous information on isomers in $^{172}$Er was limited to our proposal [6] of a $6^+$ isomer at 1501 keV, identified by only a single (assumed $M1$) 970.5-keV transition to the $6^+$ state of the ground-state band, analogous to the main decay branch of 992 keV in the known (1518-keV) $6^+$ isomer in the isotone $^{174}$Yb [7]. The mean life was suggested to be at least a few microseconds, although a definitive measurement was not possible because of the low statistics. The earlier experiment used $^{174}$Yb and $^{176}$Yb targets, but the main population probably occurred through two-proton removal from $^{174}$Yb. The advantages of the present measurements with the $^{170}$Er target are a stronger population, and also the fact that the intense transitions in the ground-state band of the target are significantly different in energy from the $^{172}$Er ground-state band transitions. In contrast, the $^{174}$Yb transitions up to the $6^+$ state are very close in energy to those in $^{172}$Er. This made it difficult in the earlier work to identify reliably other decay paths from the isomer, particularly any to the lower members of the ground-state band.

The new scheme established in the present work is provided in Fig. 5. The measurements confirm the 971-keV decay to the $6^+$ state of the ground-state band, but a much more intense path via a 134-keV transition is identified. It proceeds through a 104-keV transition, placed as the first member in a rotational band based on a short-lived isomer at 1263 keV, whose main decay is the 1008-keV transition to the $4^+$ state of the ground-state band. The branching ratios for decays from both the 1501- and 1263-keV isomeric states, the latter presumably being a $4^-$ intrinsic state related to that observed in the lighter isotopes, are given in Table I. Other branches from the $4^-$ and $6^+$ isomers proceed through states which are probably the $3^+$, $4^+$, and $5^+$ members of the $\gamma$ band. This is consistent with the excitation energy systematics and energy staggering observed in the lighter isotopes, although, in the absence of any apparent feeding to it, we have not been able to identify a $2^+$ bandhead.

Some of the evidence for the new scheme is contained in Figs. 1 and 6. The bottom panel of Fig. 1, obtained with a time gate that optimizes the shorter isomer, shows the main transitions placed in the $4^-$ band, as well as the 134-keV connection from the $6^+$ isomer. The relatively weak 153- and 291-keV transitions in this spectrum are not placed in the $4^-$ band and are much more intense in the gate on the 1008-keV $\gamma$ ray, when the time gate is shifted to a later time region, to cover the period from 150 to 800 ns (top panel of Fig. 6). These are the strongest transitions placed above the $6^+$ isomer. Also evident in this spectrum are 847- and 884-keV transitions from $^{134}$Xe, corresponding to excitation of the complementary product after the removal of two neutrons from the $^{136}$Xe beam. As will be shown later, the observation of transitions above this isomer when gating on transitions below implies a shorter mean life than the "few microseconds" proposed previously [6].

Only the 104- and 134-keV transitions appear in the middle panel of Fig. 6 which selects transitions feeding the $4^-$ isomer (delayed gate on the 1008-keV transition), and are also in the out-of-beam time region. That is, they must be located between two isomers. This (and related spectra) can be used to estimate the total conversion coefficient for the 134-keV transition. Although the 104-keV transition is placed as a cascade within the $4^-$ rotational band, and therefore will be of mixed $M1/E2$ character, the $M1$ and $E2$ total conversion

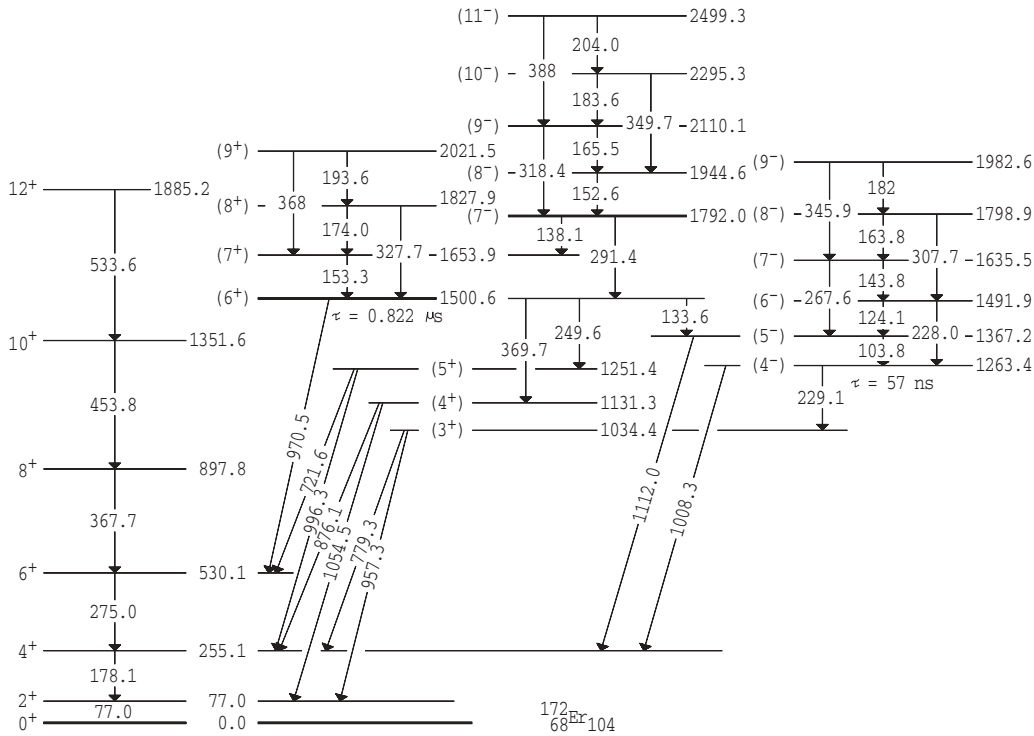


FIG. 5. Partial level scheme for $^{172}$Er as observed in the present study.

coefficients are essentially identical at this energy, with $\alpha_T = 2.56$. A delayed intensity balance then gives $\alpha_T = 0.26(3)$ for the 134-keV transition. This low value is sufficient to assign it as predominantly $E1$ in character (calculated values are 1.245 for $M1$ and 1.014 for $E2$), but the value is still somewhat higher than the expected value of $\alpha_T = 0.151$. This could be due to an issue with systematic errors in the efficiency calibration or, alternatively, an indication of a small $M2$ admixture. The $M2$ conversion coefficient is high at $\alpha_T \approx 9$. A 1% admixture of $M2$ radiation in the $\gamma$ ray intensity would be sufficient to explain the conversion coefficient, and this would correspond to an $M2$ strength of ∼0.3 W.u. This strength is only plausible if the configurations of the initial and final states involve a single orbital change, but that is not the case for the proposed assignments.

The relative intensity of the different decay paths from the $6^+$ isomer are evident in the bottom spectrum of Fig. 6. $\gamma$ rays that follow the decay of the isomer have been isolated with appropriate time and energy gates on the 153- and 291-keV $\gamma$ rays feeding it. The 970.5-keV branch directly to the ground-state band is obviously much weaker than the 134-keV branch. The 134-keV transition subsequently leads to the lower states of the ground-state band, mainly via the 104/229/957-keV sequence and the 104/1008-keV cascade.

The mean lives of the $4^-$ and $6^+$ isomeric states are obtained from fits to time spectra produced with gates above and below the level of interest (Fig. 7).

The level scheme associated with states above the isomers (Fig. 5) was confirmed through the coincidence relationships obtained from a $\gamma$-$\gamma$ matrix constructed by selecting pairs of $\gamma$ rays that precede the 229-, 957-, and 1008-keV delayed transitions (but not the 134-keV $\gamma$ ray since it is contaminated). Two bands are placed above the $6^+$ isomer, one associated with the isomer itself and a second attributed to feeding from an intrinsic state at 1792 keV, with a proposed $K^\pi = 7^-$ assignment. The rotational band property $(g_K - g_R)$ values and alignments will be discussed later, and transition strengths of decays from the isomers will be covered in the following section, but we note here that $6^+$ and $7^-$ intrinsic states are observed at very similar energies in the isotone $^{174}$Yb [7].

### E. Transition strengths and $K$ hindrances

The observed decays from each of the isomers are consistent with the proposed assignments. Of the two decays from the $4^-$ isomer, the 229-keV, $E1$ decay to the proposed $3^+$ state of the $\gamma$ band is similar in strength to the equivalent 258-keV transition in $^{170}$Er, $1.3\times10^{-7}$ and $2.3\times10^{-7}$ W.u., respectively. The branch to the $4^+$ state of the ground-state band has the same energy in both nuclei (1008.3 keV) and is much weaker, being more $K$ forbidden, although in this case, while the $^{172}$Er strength is reasonable, that in $^{170}$Er is particularly low. This seems surprising, since the configuration assigned to the $4^-$ state in $^{170}$Er involves the $i_{13/2}$ neutron and, thus, will have some Coriolis mixing, which would tend to make the transition faster rather than slower.

Four direct branches from the $6^+$ isomer are observed, the main one being the 134-keV transition to the $5^-$ level of the proposed $4^-$ band. The 134-keV transition is strongly hindered with a strength of about $10^{-7}$ W.u. (Table I). This is reasonable given its once-forbidden nature and the fact

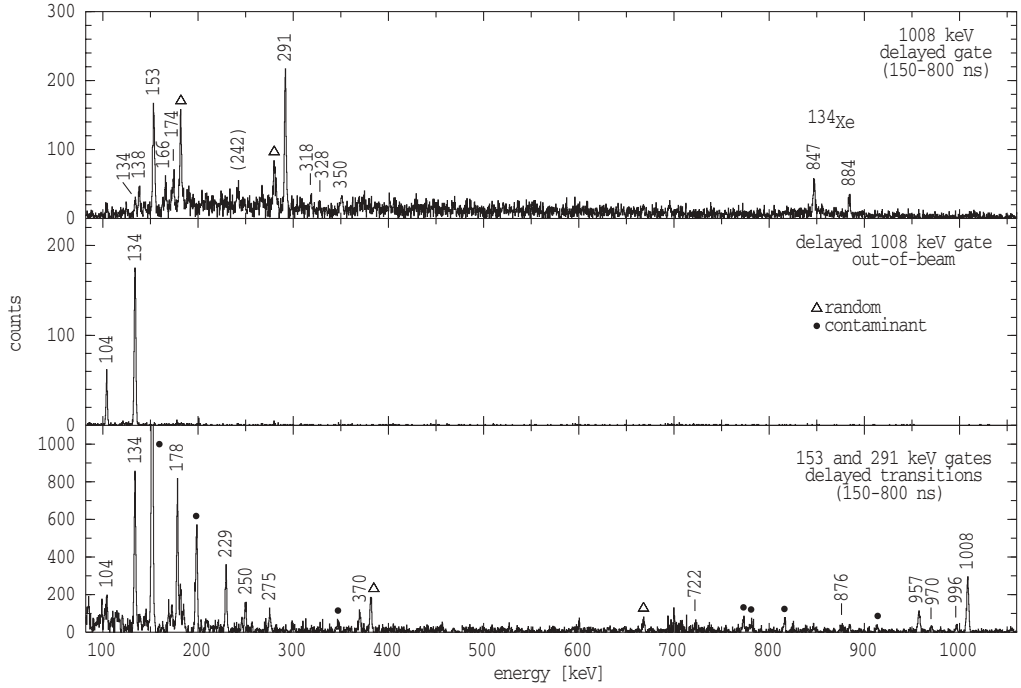


FIG. 6. Time correlated gates selecting transitions associated with the isomers in $^{172}$Er.

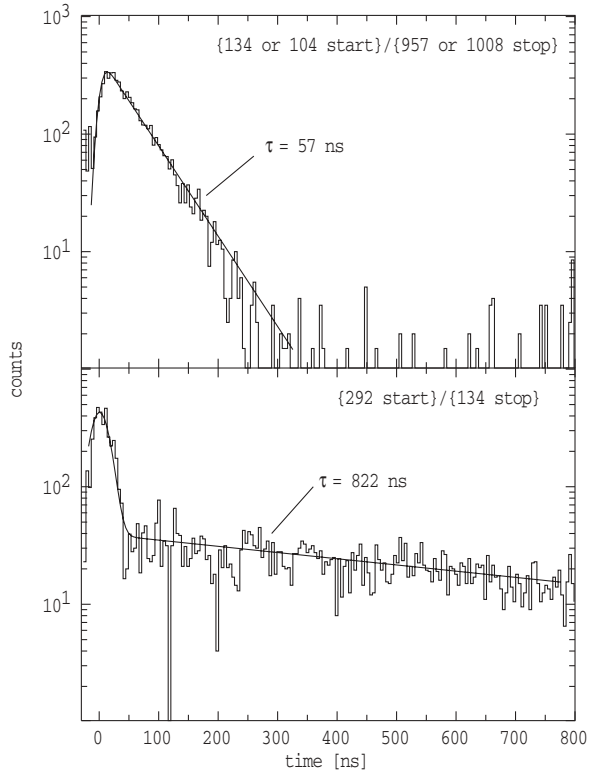


FIG. 7. Intermediate $\gamma$-$\gamma$-time spectra for $^{172}$Er. The prompt component in the lower spectrum is attributed largely to 134- and 289-keV lines that are in coincidence in the contaminant product, $^{119}$Sb.

that, as will be discussed later, it involves a two-proton to two-neutron configuration change. The $E2$ transition of 370 keV has $\nu = 2$, since the decay is to the proposed $\gamma$ band and $f_\nu = 69$, a typical value, thus indirectly supporting the $\gamma$-band assignment, as does the 250-keV $M1$ decay to the same band with $f_\nu = 176$. The five-times forbidden 970-keV, $M1$ transition to the ground-state band has $f_\nu = 56$, a much faster transition than the equivalent (992-keV) transition in $^{174}$Yb where $f_\nu = 132$ (see Ref. [7]).

A branch of interest that has not been observed is the possible 1246-keV $6^+ \rightarrow 4^+ E2$ decay to the ground-state band. The equivalent transition in $^{174}$Yb is one of the most hindered in the region with $f_\nu = 341$ [7]. An intensity limit of $\leqslant$2.3% relative to the main 134-keV branch can be placed on the 1246-keV transition in the present work, corresponding to a limit of $f_\nu \geqslant 69$, unfortunately not significant at this level, in terms of propositions about a possible $N_p N_n$ dependence leading to very highly $K$-forbidden $E2$ transition rates (see Refs. [6] and [18]).

## V. MULTIQUASIPARTICLE CALCULATIONS

Calculations of the expected multiquasiparticle spectra were carried out using an approach similar to that of Jain *et al.* [19], but with the modifications outlined in our recent publications (for example, Refs. [20–22]). The procedure involves choosing a set of single-particle levels together with the neutron and proton pairing strengths $G_\nu$ and $G_\pi$ and, in order to avoid the limitations which cause collapse of the BCS solutions in regions of low and nonuniform level densities, the use of the Lipkin-Nogami formulation for calculation of the pairing correlations.

The calculations treat the Fermi level and pairing gaps self-consistently and include particle-number conservation and blocking of occupied states for multiquasiparticle

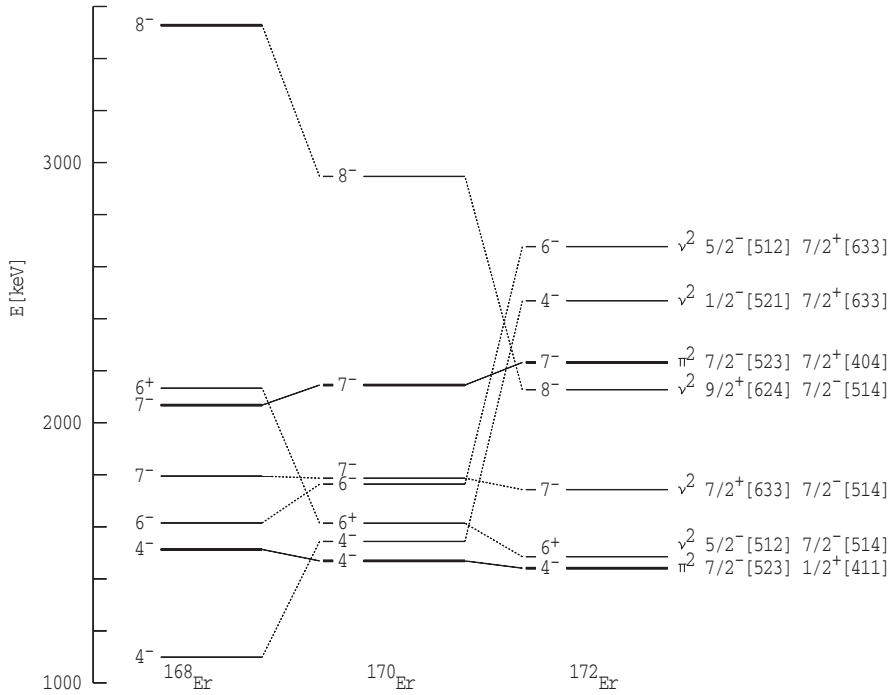


FIG. 8. Calculated two-quasiparticle states. Two-proton configurations are indicated by the bolder lines. In the $^{172}$Er case, a $7^-$ state from the $\nu^2 9/2^+[624] \otimes 5/2^-[512]$ configuration that falls essentially at the same energy as the predicted $8^-$ level has been omitted from the figure, for clarity.

configurations. For the present calculations, three oscillator shells were used for each of the neutron and proton spaces, giving 64 levels (128 states) with 28 active protons and between 60 and 64 active neutrons.

The Nilsson orbitals were calculated assuming the predicted deformations [23] of $\epsilon_2 = 0.267$ and $\epsilon_4 = 0.033$ for $^{168}$Er, $\epsilon_2 = 0.267$ and $\epsilon_4 = 0.047$ for $^{170}$Er, and $\epsilon_2 = 0.267$ and $\epsilon_4 = 0.060$ for $^{172}$Er, and provided the initial set of single-particle states. Subsequently, the single-particle energies for the neutron levels close to the Fermi surface used in the calculations were adjusted to reproduce approximately (within about 30 keV) the observed one-quasineutron states in the odd-neutron neighbors $^{167}$Er, $^{169}$Er, and $^{171}$Er. (Note that the one-quasiparticle states are calculated using the same self-consistent procedures as those used in the multiquasiparticle cases.) The lowest one-proton states are known experimentally in the neighboring $_{67}$Ho and $_{69}$Tm isotopes, with the $7/2^-[523]$ orbital forming the ground state in the former and the $1/2^+[411]$ configuration being the ground state in the latter.

The pairing strengths were taken as $G_\nu = 18.0/A$ and $G_\pi = 20.8/A$, the same values selected in evaluations of a range of Yb, Ta, and Lu isotopes (see, for example, Refs. [7,20]). Empirical residual interactions [19,22] are included in the calculation of final-state energies.

The results are presented in Fig. 8. Since the calculated quadrupole deformations are very similar across this range of isotopes, the main change being an increase in hexadecapole deformation with increasing neutron number, the predicted two-quasiproton states are approximately constant in energy, whereas the two-neutron states change rapidly. This change in the neutron structures is accentuated by the presence of the subshell gaps at $N = 98$ and $N = 104$, ($^{167}$Er has $N = 99$), since to reach $^{172}$Er involves the successive occupation of orbitals above both gaps.

## VI. CONFIGURATION ASSIGNMENTS

As is the case with the decay strengths discussed earlier, information on the underlying quasiparticle configurations is contained in the rotational band properties, in particular, rotational alignments and in-band branching ratios which are sensitive to the component orbitals.

Figure 9 presents the net alignments obtained for the observed bands with a reference chosen to produce an approximately flat curve for the ground-state band in each isotope. Following on from the earlier discussions, two alternatives ($K = 6$ or $K = 7$) are given for the 1591-keV band in $^{170}$Er.

In the case of in-band branching ratios, standard rotational model formulas can be used to extract from the measured $\Delta I = 2/\Delta I = 1$ intensities, the quantity $|g_K - g_R|/Q_0$ which is characteristic of the Nilsson configurations involved. That ratio $\lambda$ is given by

$$\lambda = \frac{(I+1)(I+K-1)(I-K-1)}{2K^2(2I-1)} \frac{E_\gamma^5(I \to I-2)}{E_\gamma^5(I \to I-1)} \frac{\delta^2}{1+\delta^2},$$

where the $\gamma$-ray energy $E_\gamma$ is in MeV, and the mixing ratio $\delta$ is

$$\delta = 0.933 \frac{E_\gamma(I \to I-1)}{\sqrt{I^2-1}} \frac{Q_0}{g_K - g_R}.$$

For multiquasiparticle configurations,

$$g_K = \frac{1}{K} \sum_i \Omega_i g_{\Omega_i}.$$

Large $g_K - g_R$ values will favor the $M1$ cascade transition over the $E2$ crossover, as will high-$K$ values. Values of $g_\Omega$ can be estimated from Nilsson wave functions for specific orbitals, and they can also be extracted from experiment for well-defined bands in nearby nuclei. A selection of these is shown in Table II for the configurations of importance here.

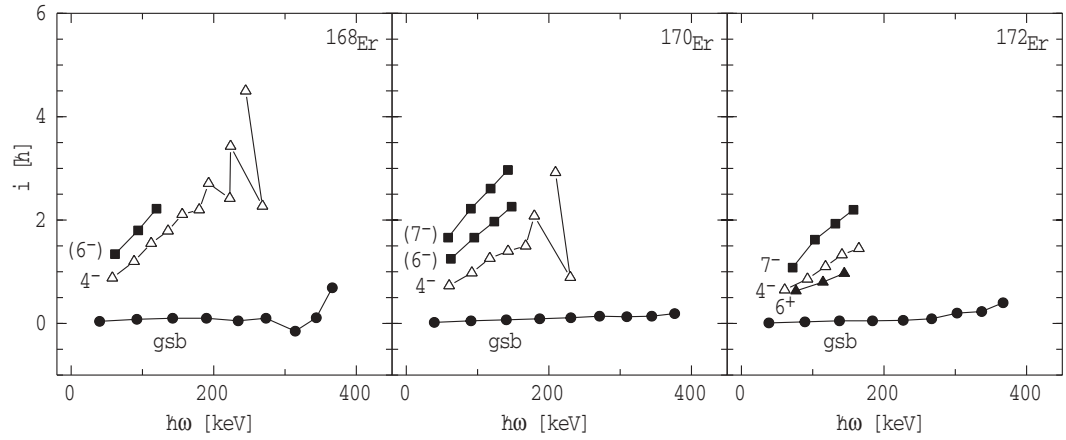


FIG. 9. Alignments as a function of rotational frequency deduced with reference parameters of $\Im_0 = 36.5$ MeV$^{-1}\hbar^2$ and $\Im_1 = 70$ MeV$^{-3}\hbar^4$ for $^{168}$Er, $\Im_0 = 37.5$ MeV$^{-1}\hbar^2$ and $\Im_1 = 60$ MeV$^{-3}\hbar^4$ for $^{170}$Er, and $\Im_0 = 38.5$ MeV$^{-1}\hbar^2$ and $\Im_1 = 60$ MeV$^{-3}\hbar^4$ for $^{172}$Er.

There are some uncertainties in the theoretical values, particularly when the component orbitals have $\Omega = 1/2$, or when the configuration is Coriolis-mixed, as in the case of the $i_{13/2}$ neutron orbitals. The theoretical Nilsson values for the former cases often change significantly with deformation because of mixing, and sometimes empirical values can only be obtained indirectly (through an analysis of two- or three-quasiparticle bands, for instance), since the branching ratios are not always accessible from one-proton rotational bands because of decoupling. For the $1/2^+[411]$ proton, we have taken the empirical value $g_\Omega = -1.75(25)$ obtained from the odd-proton nuclei, although we note that a somewhat smaller value is indicated for configurations in the odd-odd nuclei (see Ref. [24] and references therein). Together with a value of $g_\Omega = 1.25(8)$ for the $7/2^-[523]$ orbital obtained in our recent measurements on the odd-Tm isotopes [25], and $g_R = 0.31(3)$, this leads to the value of $g_K - g_R = +0.57(8)$ used below.

The value for the $4^-$ two-neutron configuration is more problematic because of the uncertainty in the effective $g_K$ value for the $7/2^+[633]$ orbital. While the calculated Nilsson value is $-0.26$ (and will be similar for all of the $i_{13/2}$ neutron orbitals), a smaller magnitude is suggested by the properties of some odd-neutron nuclei. Use of the Nilsson values for both $1/2^-[521]$ and $7/2^+[633]$ orbitals leads to a predicted value of $g_K - g_R = -0.40(4)$, whereas substitution of a lower value for the $7/2^+[633]$ orbital ($g_\Omega = -0.09$) results in $g_K - g_R = -0.25(7)$, both values being quoted in the table.

The experimental values are listed in Table III for the proposed $4^-$ bands and in Table IV for the other bands. Note that the values obtained for $^{170}$Er are about half the magnitude of those given in Ref. [3].

Consider first the $4^-$ bands: the branching ratio information only gives the magnitude of the $g_K - g_R$ values, so there are inherent ambiguities, unless the sign can be determined, for example, from the sign of the mixing ratio ($\delta$) of cascade transitions within a band. Unfortunately these are not known from the previous work on the $4^-$ bands in $^{168}$Er and $^{170}$Er, and the information is not accessible in the present experiments. However, the $g$ factor of the 1094-keV, $4^-$ isomeric state in $^{168}$Er has been reported [26] to be $g = +0.24(1)$. (Note that this is the $g$ factor, not the value of $g_K$ as was incorrectly stated in Ref. [3].) From the relationship

$$g = g_R + \frac{K^2}{I(I+1)} \times (g_K - g_R),$$

and taking $g_R = 0.31(3)$, the measured value of the $2^+$ member of the ground-state band [26], a value of $g_K - g_R = -0.09(4)$ can be extracted. The magnitude of the values of the $6^-$, $8^-$, and $10^-$ states obtained from the branching ratios (Table III) are similar, hence we can justify adopting a negative sign for all, as is plotted in Fig. 10.

Since proton configurations usually give large and positive $g_K - g_R$ values, and large magnitudes are less likely with

TABLE II. Values of $g_K$ and $g_K - g_R$ for selected configurations; see text for details.

| $K^\pi$ | Configuration | | $g_K$[a] | $g_K - g_R$[b] |
|---|---|---|---|---|
| | $\nu$ | $\pi$ | predicted | |
| $6^+$ | $5/2^-[512]\otimes 7/2^-[514]$ | | +0.06+*0.02* | −0.25−*0.29* |
| $7^-$ | $7/2^+[633]\otimes 7/2^-[514]$ | | +0.10+*0.07* | −0.21−*0.24* |
| $6^-$ | $5/2^-[512] \otimes 7/2^+[633]$ | | −0.314−*0.165* | −0.68−*0.48* |
| $4^-$ | $1/2^-[521] \otimes 7/2^+[633]$ | | −0.09+*0.06* | −0.40−*0.25* |
| $4^-$ | | $1/2^+[411] \otimes 7/2^-[523]$ | +0.88 | +0.57 |

[a]Nilsson values with semiempirical values given in italics.
[b]Taking $g_R = 0.31$.

TABLE III. Branching ratios and $(g_K - g_R)$ values for the $K^\pi = 4^-$ bands.

| $J^\pi$ | $E_\gamma(\Delta I = 1)$ (keV) | $E_\gamma(\Delta I = 2)$ (keV) | $\lambda$ | $\lvert g_K - g_R \rvert$ [a] exp. |
|---|---|---|---|---|
| $^{168}$Er; 1094 keV; $K = 4$ | | | | |
| $9^-$ | 174 | 331 | >10 | <0.15 |
| $8^-$ | 157 | 294 | 13.6(17) | $0.032^{+32}_{-32}$ |
| $7^-$ | 138 | 256 | 6.2(5) | $0.087^{+13}_{-12}$ |
| $6^-$ | 118 | 217 | 3.48(23) | $0.041^{+22}_{-24}$ |
| $^{170}$Er; 1269 keV; $K = 4$ | | | | |
| $8^-$ | 164 | 308 | 4.2(5) | $0.230^{+21}_{-18}$ |
| $7^-$ | 143 | 267 | 2.2(3) | $0.255^{+24}_{-21}$ |
| $6^-$ | 124 | 227 | 1.11(5) | $0.227^{+8}_{-8}$ |
| $^{172}$Er; 1263 keV; $K = 4$ | | | | |
| $8^-$ | 164 | 308 | 0.92(9) | $0.569^{+32}_{-28}$ |
| $7^-$ | 144 | 268 | 0.47(5) | $0.621^{+34}_{-30}$ |
| $6^-$ | 124 | 228 | 0.30(3) | $0.513^{+27}_{-24}$ |

[a]Taking $Q_0 = 7.7\ e$ b for $^{168}$Er, 7.64 $e$ b for $^{170}$Er, and 7.7 $e$ b for $^{172}$Er.

TABLE IV. Branching ratios and $(g_K - g_R)$ values.

| $J^\pi$ | $E_\gamma(\Delta I = 1)$ (keV) | $E_\gamma(\Delta I = 2)$ (keV) | $\lambda$ | $\lvert g_K - g_R \rvert$ [a] exp. |
|---|---|---|---|---|
| $^{168}$Er; 1773 keV; $K = 6$ | | | | |
| $9^-$ | 162 | 304 | <0.31 | >0.53 |
| $8^-$ | 142 | 265 | <0.25 | >0.38 |
| $^{170}$Er; 1591 keV; $K = 6$ | | | | |
| $10^-$ | 186 | 351 | 0.457(49) | $0.565^{+35}_{-29}$ |
| $9^-$ | 165 | 310 | 0.456(29) | $0.431^{+16}_{-14}$ |
| $8^-$ | 145 | 270 | 0.159(11) | $0.492^{+20}_{-18}$ |
| $^{170}$Er; 1591 keV; $K = 7$ | | | | |
| $11^-$ | 186 | 351 | 0.457(49) | $0.462^{+29}_{-24}$ |
| $10^-$ | 165 | 310 | 0.456(29) | $0.349^{+13}_{-12}$ |
| $9^-$ | 145 | 270 | 0.159(11) | $0.395^{+16}_{-15}$ |
| $^{172}$Er; 1501 keV; $K = 6$ | | | | |
| $8^+$ | 174 | 328 | 0.321(68) | $0.418^{+60}_{-44}$ |
| $^{172}$Er; 1792 keV; $K = 7$ | | | | |
| $9^-$ | 166 | 318 | 0.483(73) | $0.260^{+28}_{-23}$ |

[a]Taking $Q_0 = 7.7\ e$ b for $^{168}$Er, 7.64 $e$ b for $^{170}$Er, and 7.7 $e$ b for $^{172}$Er.

neutron configurations, we can infer (in the context of the present interpretation) a positive sign for the $^{172}$Er values. Assuming positive values for the intermediate case of $^{170}$Er, the results plotted in Fig. 10 are obtained, which is suggestive of a systematic configuration change through the isotopes, as will be quantified below. Theoretical values from Table II (with dashed lines to indicate the approximate uncertainties) are also given in Fig. 10.

By considering the experimental results together with the theoretical predictions of Fig. 8, a consistent interpretation emerges. The calculated two-neutron $4^-$ configuration in $^{172}$Er is about 1 MeV above the two-proton state (whose predicted energy matches that observed in experiment), so that little mixing is expected, consistent with the agreement observed between the experimental $g_K - g_R$ values and those predicted for the $\pi 1/2^+[411] \otimes 7/2^-[523]$ configuration (Fig. 10). At the other extreme, the (negative) $g_K - g_R$ values for $^{168}$Er are of lower magnitude than expected, consistent with a predominantly two-neutron configuration with an admixture of the (positive $g_K - g_R$) proton configuration. The admixture required to reproduce experiment is about 23% (amplitude squared). The predicted energy difference between the unperturbed $4^-$ states in $^{168}$Er is about 400 keV, which is probably reliable to within 100 keV, implying a mixing matrix element of about 190 keV. This might seem large, but documented cases of mixing matrix elements between two-proton and two-neutron states with the same value of $K$ are of this order (see Ref. [16]). For example, $|V| = 209$ keV was obtained for the $K^\pi = 6^+$ bands in $^{176}$Hf [27], while the mixing between the $K^\pi = 8^-$ bands in $^{178}$Hf [28–30] corresponds to $|V| = 158$ keV. In the intermediate case of $^{170}$Er, the experimental $g_K - g_R$ values imply approximately equal two-neutron and two-proton components, consistent with the prediction that the two configurations would give rise to approximately degenerate unperturbed states.

With respect to other two-quasiparticle states and the comparison between theory and experiment in $^{168}$Er, a $K^\pi = 6^-$ state from the $\nu^2 5/2^-[512] \otimes 7/2^+[633]$ configuration is predicted to lie about 50 keV above the $4^-$ bandhead, although the candidate state at 1773 keV is nearly 700 keV higher. The lower limits on the observed $g_K - g_R$ values for the $9^-$ and $8^-$ band members are in agreement with the large (negative) value predicted (Table II), and the relatively high alignment (see Fig. 9) concurs with the presence of an $i_{13/2}$ neutron in the configuration.

In $^{170}$Er, both $6^-$ and $7^-$ intrinsic states, the latter from the $\nu^2 7/2^-[514] \otimes 7/2^+[633]$ configuration, are predicted at similar energies, and an earlier discussion (Sec. IV E) focused on alternative $6^-$ and $7^-$ assignments for the 1591-keV intrinsic state. However, the predicted $g_K - g_R$ value for the $7^-$ configuration is significantly smaller than the experimental values, while that for the $6^-$ alternative is in reasonable agreement with theory (both experimental alternatives are listed in Table IV). Again, the alignment is consistent with the proposed configuration. In contrast to the situation in $^{170}$Er, the $\nu^2 5/2^-[512] \otimes 7/2^+[633]$, $6^-$ configuration gives rise to a strongly populated and long-lived isomer at 1551 keV in the isotone $^{172}$Yb [31], the difference being that equivalent

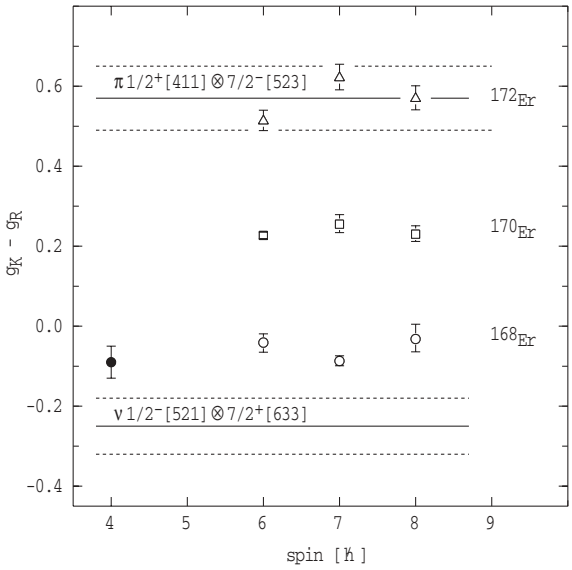


FIG. 10. Measured and predicted $g_K - g_R$ values for the $4^-$ bands. As discussed in the text, the experimental signs are assumed, except for case of the $^{168}$Er, $4^-$ state, where the value is deduced from the measured $g$ factor. All other experimental values are from the $\gamma$-ray branching ratios (Table III).

decay paths are not available in $^{172}$Yb, since the $4^-$ structure is located at a higher energy (1641 keV) in that nucleus. Several other candidates for intrinsic states are found in $^{170}$Er, but with largely uncertain spin assignments, in particular the 1943-keV state and the pair of states at 2168 and 2432 keV. The latter pair could be candidates for the $7^-$ two-proton state and the $8^-$ two-neutron state that is predicted to fall rapidly through the isotopes, but there is insufficient information to test this.

Because of the low population, it was also only possible to obtain a value for one state in each of the 1501- and 1792-keV bands in $^{172}$Er. Nevertheless, these are very similar to the values of $|g_K - g_R| = 0.437(6)$ and $|g_K - g_R| = 0.261(7)$ obtained for the $6^+$ and $7^-$ bands in $^{174}$Yb [7], supporting the proposed correspondence with the isotone. As noted previously [7], the observed value for the $6^+$ band is higher than the predicted value for the assigned configuration (see Table II), but the value for the $7^-$ band from the branching ratios (Table IV) is in good agreement with the predicted value for the $\nu^2 7/2^-[514] \otimes 7/2^+[633]$ configuration.

Note that the alignment for the $4^-$ band in $^{172}$Er is similar to the low value observed for the $6^+$ band in the same nucleus (Fig. 9), consistent with the absence in this case of an $i_{13/2}$ neutron in the $6^+$ two-neutron configuration and the assignment of a two-proton configuration to the $4^-$ band, although this is not a strong argument, since the alignment differences are not very pronounced.

Finally, one possible surprise is the absence of a $6^+$ intrinsic state in $^{170}$Er. The calculations predict a $6^+$ state at relatively low energies, between the $4^-$ and $6^-$ states. Whether such a state in $^{170}$Er would be an isomer would depend on the possible decay paths, and the energy might simply be underestimated, given the rapid rise of this configuration with decreasing neutron number.

## VII. SUMMARY

New excited states have been identified in the range of the stable and neutron-rich isotopes $^{168}$Er, $^{170}$Er, and $^{172}$Er with Gammasphere and inelastic excitations induced by energetic $^{136}$Xe beams. The improved energy resolution and sensitivity compared to previous work has allowed more extensive level schemes to be established and has revealed low-energy transitions whose presence could have compromised the interpretation of $\gamma$-ray branching ratios in earlier work. These new results, together with the identification of a $4^-$ isomer and its associated rotational band in $^{172}$Er, lead to the conclusion that the main configurations involved in producing a $4^-$ isomer as a function of neutron number correspond to an 80%/20% combination of the competing two-neutron and two-proton configurations in $^{168}$Er, approximately equal mixing in $^{170}$Er, and a dominant two-proton structure in $^{172}$Er. This deduction is supported by the experimental band properties and the expectations from multiquasiparticle calculations. The level scheme for $^{172}$Er has been considerably extended, including identification of the aforementioned $K^\pi = 4^-$ structure, which provides the main decay path for the previously proposed two-quasineutron $6^+$ isomer at 1501 keV. The lifetime of the $6^+$ isomer is measured as $\tau = 822(90)$ ns, the associated rotational band has been observed, as has feeding from a higher-lying $K^\pi = 7^-$ band with a bandhead at 1792 keV. Although not as extensive, the $6^+$ and $7^-$ structures are strikingly similar to the two-quasiparticle structures observed in the isotone $^{174}$Yb. The systematics of the observed two-quasineutron and two-quasiproton intrinsic states are in good agreement with calculations.

## ACKNOWLEDGMENTS

The authors thank R. B. Turkentine for producing the target and the staff of the ATLAS accelerator facility for their assistance in various phases of the experiment. This work is supported by the Australian Research Council Discovery program (DP0986725) and the US Department of Energy, Office of Nuclear Physics, under Contract No. DE-AC02-06CH11357 and Grant No. DE-FG02-94ER40848.

[1] V. S. Shirley, Nucl. Data Sheets **71**, 261 (1994).
[2] C. M. Baglin, Nucl. Data Sheets **96**, 611 (2002).
[3] C. Y. Wu, D. Cline, M. W. Simon, R. Teng, K. Vetter, M. P. Carpenter, R. V. F. Janssens, and I. Wiedenhöver, Phys. Rev. C **68**, 044305 (2003).

[4] C. Y. Wu, D. Cline, M. W. Simon, R. Teng, K. Vetter, M. P. Carpenter, R. V. F. Janssens, and I. Wiedenhöver, Phys. Rev. C **61**, 021305(R) (2000).
[5] C. Y. Wu, D. Cline, M. W. Simon, R. Teng, K. Vetter, M. P. Carpenter, R. V. F. Janssens, and I. Wiedenhöver, Phys. Rev. C **70**, 014313 (2004).
[6] G. D. Dracoulis *et al.*, Phys. Lett. B **635**, 200 (2006).
[7] G. D. Dracoulis *et al.*, Phys. Rev. C **71**, 044326 (2005); **73**, 019901(E) (2006).
[8] G. D. Dracoulis *et al.*, Phys. Rev. C **79**, 061303(R) (2009).
[9] R. Broda, M. A. Quader, P. J. Daly, R. V. F. Janssens, T. L. Khoo, W. C. Ma, and M. W. Drigert, Phys. Lett. B **251**, 245 (1990).
[10] R. Broda, C. T. Zhang, P. Kleinheinz, R. Menegazzo, K.-H. Maier, H. Grawe, M. Schramm, R. Schubart, M. Lach, and S. Hofmann, Phys. Rev. C **49**, R575 (1994).
[11] J. F. C. Cocks *et al.*, J. Phys. G: Nucl. Part. Phys. **26**, 23 (2000).
[12] R. Broda, J. Phys. G: Nucl. Part. Phys. **32**, R151 (2006).
[13] R. V. F. Janssens and F. S. Stephens, Nucl. Phys. News **6**, 9 (1996).
[14] M. Cromaz, T. J. M. Symons, G. J. Lane, I. Y. Lee, and R. W. MacLeod, Nucl. Instrum. Methods Phys. Res. Sect. A **462**, 519 (2001).
[15] E. P. Grigoriev and I. A. Gladkova, Phys. At. Nucl. **63**, 705 (2000).
[16] G. D. Dracoulis *et al.*, Phys. Rev. Lett. **97**, 122501 (2006).
[17] C. J. Gallagher, Nucl. Phys. **16**, 215 (1960).
[18] P. H. Regan, F. R. Xu, P. M. Walker, M. Oi, A. K. Rath, and P. D. Stevenson, Phys. Rev. C **65**, 037302 (2002).
[19] Kirain Jain, O. Burglin, G. D. Dracoulis, B. Fabricius, N. Rowley, and P. M. Walker, Nucl. Phys. A **591**, 61 (1995).
[20] F. G. Kondev, G. D. Dracoulis, A. P. Byrne, T. Kibédi, and S. Bayer, Nuc. Phys. A **617**, 91 (1997).
[21] F. G. Kondev, G. D. Dracoulis, A. P. Byrne, and T. Kibédi, Nucl. Phys. A **632**, 473 (1998).
[22] F. G. Kondev, Ph.D thesis, Australian National University, 1996.
[23] P. Möller, J. R. Nix, W. D. Myers, and W. J. Swiatecki, At. Data Nucl. Data Tables **59**, 185 (1995).
[24] R. O. Hughes, G. J. Lane, G. D. Dracoulis, T. Kibédi, P. Nieminen, and H. Watanabe, Phys. Rev. C **77**, 044309 (2008).
[25] R. O. Hughes, G. J. Lane, G. D. Dracoulis, T. Kibédi, P. Nieminen, and H. Watanabe (to be published).
[26] A. Furusawa, M. Kanazawa, and S. Hayashibe, Phys. Rev. C **21**, 2575 (1980).
[27] T. L. Khoo, J. C. Waddington, and M. W. Johns, Can. J. Phys. **51**, 2307 (1973).
[28] F. W. N. de Boer, P. F. A. Goudsmit, B. J. Meijer, J. C. Kapteyn, J. Konijn, and R. Kamermans, Nucl. Phys. A **263**, 397 (1976).
[29] T. L. Khoo and G. Løvhøiden, Phys. Lett. B **67**, 271 (1977).
[30] S. M. Mullins, G. D. Dracoulis, A. P. Byrne, T. R. McGoram, S. Bayer, W. A. Seale, and F. G. Kondev, Phys. Lett. B **393**, 279 (1997); **400**, 401(E) (1997).
[31] P. M. Walker, S. R. Faber, W. H. Bentley, R. M. Ronningen, and R. B. Firestone, Nucl. Phys. A **343**, 45 (1980).